

# From Antenna Stents to Wireless Geiger Counters: The Promise of Electrical Micro-Discharges in the Fabrication and Operation of Microsensors

Yogesh B. Gianchandani

Engineering Research Center for Wireless Integrated Microsystems,  
and Solid State Electronics Laboratory,  
University of Michigan, Ann Arbor, MI 48109-2122, USA

## Abstract

Micro-scale electrical discharges can be useful in both manufacturing contexts and sensing modalities. With regard to manufacturing, they provide structural and material diversity: microplasmas ignited between thin film metal patterns permit localized etching and deposition, whereas micro-arcs permit stainless steel and other bulk metals. Micro-electrodischarge machining has been used for the lithography-compatible fabrication of “smart stents” that are integrated with pressure sensors. It has also been used to embed sensors at the tip of biopsy needles. With regard to sensing modalities, spectroscopic detection of chemicals in both gas and liquid phase has been explored. For example, discharge spectroscopy has been used to detect inorganic contaminants such as lead and chrome in water. The converse application has also been reported: salts dissolved in aqueous sample are used to tune the emission spectrum, which is subsequently filtered and used as an inexpensive UV source for the fluorescent detection of biochemicals. Gas-phase discharges are used for radiation sensing by Geiger counters and related micromachined devices. It has been shown that the RF emissions associated with these discharges are in the UWB spectrum, and can be detected by common AM/FM radios, creating some interesting opportunities for wireless networking.

## I. INTRODUCTION

Plasma-based processes are now routinely used in the fabrication of micro-electronic circuits and microsystems. While the primary applications are in dry etching of silicon and related compounds and low-temperature deposition of dielectric materials, other uses also exist, such as cleaning of wafers and activation of surfaces in preparation for bonding. There are both similarities and differences between such macro-scale plasmas and the electrical micro-discharges that are the subject of this paper. For example, conventional plasma systems that are used extensively in semiconductor manufacturing typically operate at 10-500 mTorr pressure, and power densities of 10-500 mW/cm<sup>2</sup>. The energy is delivered in the form of and RF or microwave radiation, and the plasma extends almost uniformly across a chamber in which one or more wafers are placed. Spatial selectivity (e.g., for features to be etched) is provided by a masking layer such as photoresist.

In contrast, micro-discharges are spatially localized to a region of the sample that is typically within a few hundred microns of the electrodes. The sample itself typically serves an electrode or provides a substrate for thin-film electrodes. The operating pressure is often much higher than it is for conventional plasmas, ranging from 100 mTorr to atmospheric pressure. The shortened mean free path of gas molecules at higher pressures helps to improve the natural confinement of the discharge. The confinement of the discharge permits the energy densities of microplasmas to be in the range of 1-10 W/cm<sup>2</sup>. While micro-discharges may be excited by RF power, DC power or pulsed DC power is also used. The overall ionization levels are modest, resulting in electron and ion densities in the range of 10<sup>9</sup>-10<sup>11</sup> cm<sup>-3</sup>. However, the average electron energy in the vicinity of the cathode can be 100-200 eV [1-3]. Since the microplasmas are driven primarily by secondary electrons from the cathode, the glow region tends to be localized to the immediate vicinity of the cathode. This is quite different from what is observed in larger, more conventional plasmas, and can be a useful feature for some applications. As the current density in a discharge is increased, it progresses from a normal glow plasma discharge, to the abnormal glow region, and finally changes to an arc, which provides very current density ( $\approx 1$  A/cm<sup>2</sup>) but sustains a relatively small voltage drop. Sparks are transient discharges that have even higher current density ( $\approx 1$  KA/cm<sup>2</sup>). One of the primary challenges in using micro-discharges for sensing and actuation lies in controlling their voltage, current, and energy distribution over time and space.

The next section describes some examples to illustrate the value of microdischarges to manufacturing, and the following one describes cases in which the microdischarges participate in the transduction.

## II. MANUFACTURING

Stated in a general way, two of the most important research goals for lithography-compatible microfabrication techniques include the facilitation of structural complexity and material diversity. Both of these can be important for the future development of biomedical devices and microsystems, such as analytical tools and implantable sensors. Micro-discharges can contribute toward both of these goals. For example, microplasmas can facilitate certain types of structural complexity and micro arcs can facilitate material diversity.

### Microplasmas

One aspect of structural complexity is being able to etch materials to a variety of depths (perhaps dozens) in a single

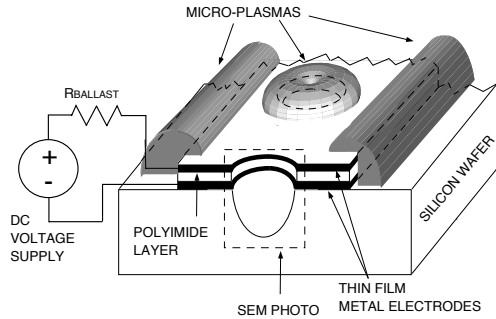


Fig. 1: Schematic illustrating the generation of an in-situ microplasma [4].

microstructure. A conceivable application may be sorting of biological species by size within a microfluidic system. In conventional etching schemes, implementing a structure like this would require dozens of masking steps. In contrast to traditional techniques, an *in-situ* microplasma is formed by applying DC power between two thin-film metal electrodes patterned on the Si substrate and separated by a dielectric spacer (Fig. 1). This arrangement not only shields the substrate from applied electric fields, but also permits the use of DC power, eliminating the tuning requirements of RF plasmas [4]. The tri-layer stack also serves as the hard mask for etching patterns that are smaller than the confinement limit of the microplasma. The stack is fabricated by a two-mask process. Multiple microplasmas with different etch characteristics may operate sequentially on different regions of a wafer, and simultaneous operation is also possible for many cases. Past work has demonstrated that etch rates  $>17 \mu\text{m}/\text{min}$ . and through-wafer etches can be achieved using  $\text{SF}_6$ . The etch profiles obtained indicate that varying degrees of anisotropy can be achieved using conventional approaches of selecting plasma conditions, gases, and wafer temperature.

Microplasmas can also provide structural diversity by spatially plasma-enhanced chemical vapor deposition (PECVD). In the effort described in reference [5], microplasmas were excited between thin-film Ti electrodes patterned on a glass microchip. Arrayed electrodes arrangements were used in which multiple cathode elements shared a single anode. With plasma glow confined to the regions directly over the energized cathodes, the deposition was localized to these regions. A silane ambient permitted Si to be deposited on the cathode elements at rates approaching those of conventional PECVD of Si. This work also showed that by varying power and pressure, the isolated elements in a cathode array could be activated through the plasma itself, eliminating the need for direct wiring of each electrode.

#### $\mu\text{EDM}$ Technology

On the issue of material diversity, many bulk metals, e.g. steel and Pt-Rh, are attractive because of their mechanical and chemical properties. Unfortunately, most metals are neither conveniently etched by plasmas nor

easily deposited by electroplating, chemical vapor deposition, or other methods conventionally used in microfabrication. Micro-electro-discharge machining ( $\mu\text{EDM}$ ) is an attractive alternative that can be used to cut any electrically conductive material, including permanent magnets. It involves the sequential discharge of electrical pulses between a microscopic electrode and the workpiece while both are immersed in dielectric oil [6]. The pulse discharge timing is controlled by a simple RC circuit. The electrode is conventionally a cylindrical metal element that is  $5\text{-}300 \mu\text{m}$  in diameter. The electrodes themselves are individually shaped by using a  $\mu\text{EDM}$  technique known as wire electro-discharge grinding (WEDG) [7]. The use of a single electrode that is rastered or scrolled across the sample surface can be helpful for rapid prototyping because it does not require the use of masks.

Although it has been commercially used for applications such as ink-jet nozzle fabrication, this traditional  $\mu\text{EDM}$  method is limited in throughput because it is a serial process. Batch mode  $\mu\text{EDM}$ , that uses lithographically-fabricated electrode arrays, can overcome this limitation [8-10]. Electroplated Cu electrodes fabricated on a Si substrate provide spatial multiplicity in the electrical discharges (Fig. 2). However, if they are all connected in parallel to the same pulse generation circuit, only one tends to fire at any given moment. By separating arrayed electrodes into segments that are independently controlled, it is possible to achieve both spatial and temporal multiplicity, providing machining throughput that is orders of magnitude higher than is possible by a serial approach [10]. This can be facilitated, in part, by utilizing the parasitic on-chip capacitance between the electrodes and the Si substrate as a design component within the pulse timing circuit. Not only does this provide a compact solution, but the resulting elimination of the parasitic nature of the capacitance provides superior control over the size and timing of the pulses, improving the precision of the machining and reducing cross-talk between electrodes.

#### Stents and Antenna Stents

The  $\mu\text{EDM}$  method has been used in the recent past to fabricate stents [11-12]. Stents are mechanical devices that are chronically implanted into arteries in order to physically expand and scaffold blood vessels that have been narrowed by plaque accumulation. Although they have found the greatest use in fighting coronary artery disease, stents are also used in blood vessels and ducts in other parts of the body. These include iliac,

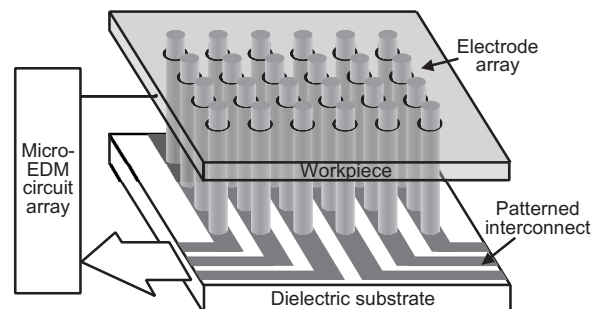
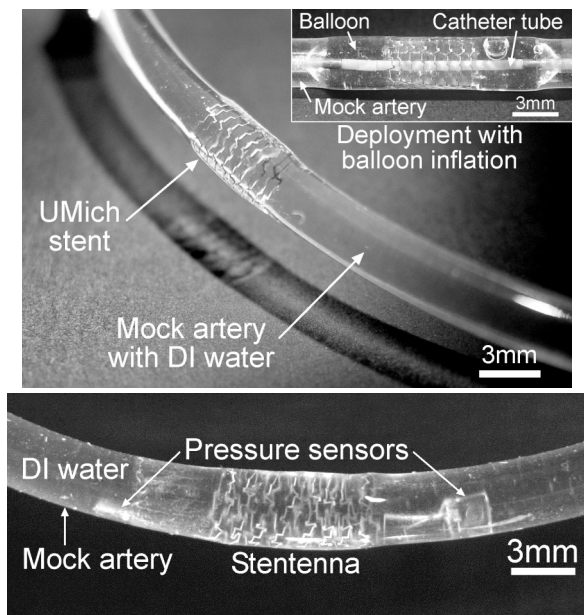


Fig. 2: The concept of batch mode  $\mu\text{EDM}$  [10].

carotid, and renal arteries, biliary ducts and ureters. The vast majority of coronary stents are made by laser machining of stainless steel tubes, creating mesh-like walls that allow the tube to be expanded radially with a balloon that is inflated during the medical procedure, known as balloon angioplasty. A lithography-compatible method for fabricating these devices would be useful for the purpose of integrating sensors and sensing materials onto them. (It would also permit such 3D structures and assembly methods to be incorporated into the portfolio of micromachining techniques being used for other devices.) This type of ability to monitor pressure and flow can be useful because re-narrowing (restenosis) often occurs following a stenting procedure, and intraluminal wireless sensors for pressure or flow can be used in monitoring of the patency of the lumen.

Wireless pressure sensors have also been reported in association with stent grafts used to repair abdominal aortic aneurysms [13]. However, in this case the sensors are located in the aneurysm, not within the stent or path of blood flow. For this reason, miniaturization and integration with the stent is not essential, and sensors of 1-2 cm length can be accommodated in this application.



**Fig. 3:** (a) Stent fabricated from planar steel foil using  $\mu$ EDM and deployed within a mock artery using balloon angioplasty [11]. (b) The antenna stent coupled with two capacitive pressure sensors [12].

Reference [11] describes a lithography-compatible approach to the design and fabrication of stents based on use of planar stainless steel foil. The devices were intended to be compatible with standard stenting tools and procedures, and used flexural designs that did not require any bonded or welded seams. In the planar form, the patterns were cut into 50- $\mu$ m thick stainless steel foil, and

consisted of involute bands between a pair of side-beams. In assembling the device, a deflated angioplasty balloon was threaded alternately above and below the bands, and then expanded by a normal angioplasty procedure. Stents were expanded in two ways: inside mock arteries (Fig. 3a) and without external confinement (i.e. free-standing). Free-standing stents exhibited diameter variations of  $<\pm 4\%$ , almost zero radial recoil after deflation of the balloon, and longitudinal shrinkage of  $<3\%$  upon expansion. Loading measurements demonstrated that the designs had radial strength similar to commercial stents.

In a further extension of this technology, a modified version of the stent was used as an inductive element in conjunction with a micromachined capacitive pressure sensor [12]. The inductive antenna stent (stentenna) was 20 mm in length and had 3.5-mm expanded diameter. It was coupled with capacitive elements to form resonant LC tanks that could be telemetrically queried (Fig. 3b). The resulting LC tanks are deployed inside silicone mock arteries using standard angioplasty balloons and used to wirelessly sense changes in pressure and flow. Using water as the test fluid, the resonant peaks shifted from about 208 MHz to 215 MHz as the flow was changed from 370 to 0 mL/min.

A variation of the fabrication approach for these stents uses strategically located narrowed beams or “necks” in the pattern, which serve as breakable links. As the links are broken during the balloon expansion process, the structure can be transformed from planar mesh to a helical shape. While breakable links are not necessarily suitable for stents, they provide additional freedom in customizing the mechanical and electrical properties of these devices for other applications.

#### Biopsy Tools

The ability of  $\mu$ EDM to pattern steel has also been useful in embedding sensors into biopsy tools. The initial work described in [14] was motivated primarily by fine needle aspiration (FNA) of thyroid nodules. While thyroid cancer results in  $<1\%$  of cancer deaths, its clinical diagnosis can be very challenging. This is because malignant tumors must be differentiated from benign nodules. Since thyroid nodules can be observed in about 20% of the general US population, and the ultrasound characteristics of benign and malignant nodules are similar, FNA biopsy is usually required to make a final diagnosis. This is typically performed with a (20-27 gauge) needle attached to a 10 mL syringe for suction of thyroid tissue, which is then examined by a cytologist.

The biopsy is challenging because of the precision required in recovering a sample from the small target volumes. To aid this, conventional ultrasound imaging is performed in real time, especially for those nodules that are difficult to palpate or contain complicated solid and cystic areas. This adds significant complexity, requiring special training and equipment that only limited hospitals can afford, yet is not always effective. At least 2-5% of FNAs are read as non-diagnostic because of improper sampling. A biopsy needle that can detect different tissue planes or variations of densities (e.g., solid vs. cystic) can make the detection of this easily cured cancer not only more accurate, but more widely accessible.

In this work, a piezoelectric sensor was integrated into a cavity at the tip of the biopsy needle (Fig. 4). The  $\mu$ EDM process was used in two ways. First, it was used to form the 300  $\mu$ m diameter cavity near the tip of a stainless steel biopsy needle in which the sensor would be located. Second, it was used to form the piezoelectric sensor from lead zirconate titanate (PZT) using a customized process. More specifically,  $\mu$ EDM was used to form a steel tool that was subsequently used for batch-mode micro ultrasonic machining ( $\mu$ USM) of bulk PZT ceramic. This process is described in some detail in [15]. The resulting sensor was 50  $\mu$ m thick and 200  $\mu$ m in diameter. Devices were tested in materials that mimic the texture of human tissue in the training of physicians, and were separately tested with porcine fat and muscle tissue. The magnitude and frequency of a resonant peak shows tissue-specific characteristics that are related to the acoustic impedance of the local tissue as the needle advances into the sample. For example, in the porcine tissue sample, the magnitude and peak frequency respectively change from  $\approx 2118 \Omega$  and  $\approx 163$  MHz to  $\approx 562 \Omega$  and  $\approx 150$  MHz as the needle moves from fat to muscle tissue.

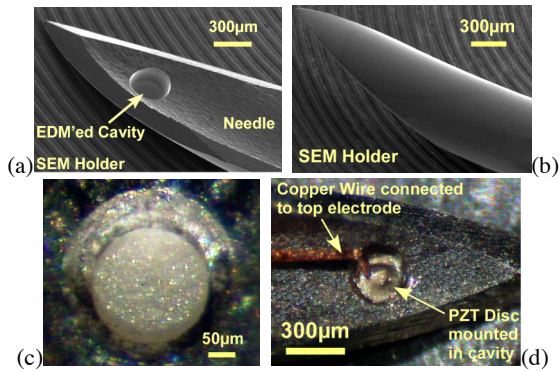


Fig. 4: SEM images of  $\mu$ EDM'd syringe needle tip with the cavity for mounting PZT sensor: (a) inner side view; (b) outer side view. Optical images of: (c) a PZT disc mounted in the cavity at the tip of a syringe needle. Cavity diameter: 300  $\mu$ m, depth: 150  $\mu$ m. Corresponding diaphragm thickness: max. 36  $\mu$ m, min. 10  $\mu$ m; (d) Fabricated device prior to epoxy seal. A coated copper wire is used to make connection to the top electrode of the PZT disc. The stainless steel needle body is used as ground [15].

### III. SENSING

The contexts in which electrical microdischarges have been directly used in sensing are related to chemical detection (in both liquid and gaseous phase) and radiation sensing.

#### Water Quality

Presently, water quality assessment is a relatively elaborate process, requiring sample transportation and laboratory analysis at centralized locations. With threats to potable water sources from industrial and biochemical pollutants, diagnostic tools that can provide rapid on-site tests for contaminants are of significant interest. A liquid

electrode spectral emission chip (LED-SpEC) was reported in [16] for the detection of trace contaminants in water by spectroscopy of micro glow discharges. Based on a concept that was first described in [23], the device was fabricated by a four mask process, that provided a reservoir and channels in a glass substrate, along with electrodes that bias the water sample. Liquid from the cathode is sputtered into the discharge, for spectroscopic detection of impurities. Using a commercial spectrometer, Na concentration  $< 10$  ppm, and Pb concentration of 5 ppm, and Al and Cr concentrations of 10 ppm were measured. The ratio of Na spectral intensity to that of ambient  $N_2$  is shown to be a suitable measure of Na impurity concentration over several orders of magnitude. Addition of  $HNO_3$  to lower the pH of the liquid solution increases this ratio by almost an order of magnitude. Other configurations for the same device concept are reported in [17, 18, 24, 25].

#### Fluorescent Detection

By intentionally doping the water sample, the same basic device concept can serve as a customizable optical source for fluorescent detection of biochemicals. Fluorescence detection is a widely used technique in medical diagnostics and biochemical analysis. Fluorescent dyes are sometimes used to chemically label the analyte of interest, which may range from DNA to compounds like glucose, ATP, RNA, proteins, oxygen, carbon dioxide in the cellular microenvironment. Many proteins are fluorescent even without the presence of a dye, and changes in this intrinsic or direct fluorescence can be indicative of structural transformations. The intrinsic fluorescence of such proteins and peptides is due to the presence of tryptophan, tyrosine or phenylalanine, which are fluorescent amino acids. In contrast to the excitation and emission wavelengths for the SYBR green dye, which are in the visible portion of the spectrum, these three have absorption peaks over 250-290 nm and emission peaks over 280-350 nm, all in the deep ultra-violet (UV) region. There are relatively few options for cheap and disposable sources of light at such wavelengths because solid-state sources such as light-emitting diodes and lasers are

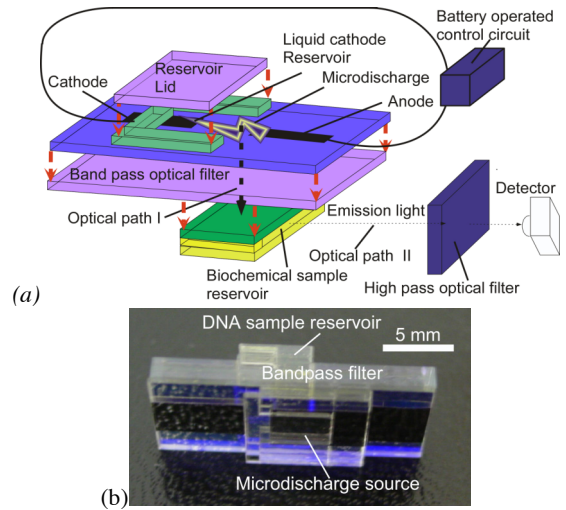


Fig. 5: (a) Configuration of a UV source based on spectral emission from a doped liquid cathode. (b) Fabricated device [19].

primarily available for somewhat longer wavelengths and are not necessarily tunable.

A stacked microchip that integrates a discharge-based microfluidic wavelength-tunable optical source, a biochemical sample reservoir and optical filters was reported in [19]. The device configuration is illustrated in Fig. 5. The characteristic line spectra, which arise from energetic transitions of the metal ions that are sputtered into the glow region of the discharge, are optically filtered and guided to the biochemical sample that resides in a separate on-chip reservoir. For DNA fluorescence, a barium chloride solution was used to emit light at 454 and 493 nm. For tryptophan fluorescence, the cathode contained lead (II) nitrate solution to provide a 280 nm emission.

#### Gas Sensors

Gas sensing devices that measure impurities by ionizing the sample and measuring the spectra have the potential for very sensitive measurements, and the advantages of a large database of spectral characteristics. Mass spectrometers, which measure the ratio of ion mass-to-charge are often used for detecting gases. In particular, quadrupole mass spectrometers have an ion source, an electrostatic lens with four poles to focus the ion flow, and an array of detectors to measure the spatial deflection of ions, which is proportional to their charge-to-mass ratios. Ions with smaller mass to charge ratios are deflected more. Using micromachining technology, a quadrupole mass spectrometer has been developed with 500- $\mu\text{m}$  diameter electrodes [20]. Time of flight mass spectrometers ionize gas atoms in bursts, accelerate the ions electrostatically, and measure their time of flight, which is a function of ion mass. Ion mobility mass spectrometers, which have the capability of operating at atmospheric pressure, exploit differences in the mobilities of species in the presence of a background gas. A miniaturized RF ion mobility spectrometer has been reported in [21]. Other efforts have been directed at miniaturizing inductively coupled plasmas to be utilized for gas spectroscopy [22]. A handheld gas sensing instrument based on optical emission spectroscopy of discharges between planar microelectrodes was reported in [26]. This instrument has an interchangeable chip that permits it to be used for liquid phase samples as well. One of the challenges in discharge-based gas sensing, in general, is rapid electrode wear. It has been shown in [27], that even in planar electrode arrangements, the power in a discharge can be suppressed by the use of a high-impedance gate electrode between the anode and cathode, which can improve device longevity.

#### Wireless Geiger

Environmental monitoring is emerging as a significant driver of microsystems technology. For applications ranging from industrial control to homeland security, there is interest in microsystems that can provide a first alert for various environmental variables, including radiation. Solid-state detectors for beta particles exist, but they

typically require cryogenic cooling to distinguish radiation type and energy, and are susceptible to radiation damage [28-30]. Another type of device uses pixelated silicon structures at room temperature to provide spatial imaging of beta particle flux [31]. Geiger counters, however, are the preferred sensors for detecting beta radiation [32]. Conventional Geiger counters are commonly hand-held devices, with an electrode pair in partial vacuum, biased at 500-1000 V. A thin window permits the entry of beta particles, which ionize the gas in the tube, resulting in avalanche breakdown, and registering individually as “counts”. In general, these gas-based detectors can be reliable, temperature insensitive, require only simple circuitry, and measure over a wide range of radiation species and energies.

A micromachined Geiger counter fabricated from stacked glass and Si wafers was reported in [33]. A single die of 2 cm<sup>2</sup> had 6 independent chambers ranging in size from 8x8 mm<sup>2</sup> to 1x3 mm<sup>2</sup>. Helium and neon, which have different voltage bias requirements, were separately evaluated as background gases. In tests the device was found to detect incident beta particles from a Uranium-238, and calibrated <sup>90</sup>Sr, <sup>60</sup>Co, and <sup>204</sup>Tl sources, of 0.1-1  $\mu\text{Curie}$  strength. In the D-microGeiger, incident beta particles pass through two independent cavities that are separated by a glass barrier, which provides calibrated energy absorption. By comparing the counts in the two cavities, information about the energy of the radiation is determined. This provides assistance in determining the chemical nature of the isotope, not just the presence of radiation.

Gas discharges across relatively large gaps (on the order of cm) have been employed in the past with spark gap transmitters for communication applications dating back to Marconi in the mid-1890's. Since Geiger counters utilize gas discharges, this mechanism presents the possibility of detecting radiation in a wireless manner, possibly for networked applications. Networked radiation sensors can be envisioned for monitoring public and inaccessible terrains. The measurement of RF transmissions from a micromachined Geiger counter was reported in [34]. An alternate configuration (Fig. 6) that utilizes permanent magnets to enhance the transmissions in the 2.0-2.8 GHz frequency range was reported in [35].

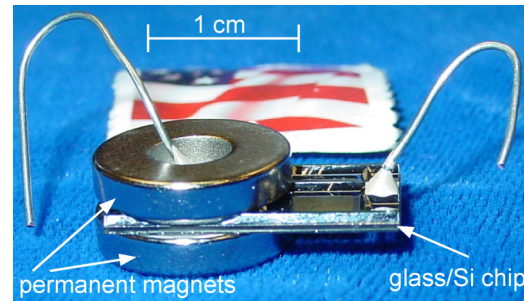


**Fig. 6:** Photograph of a wireless micro-Geiger device [35].

## IV. CONCLUSIONS

These efforts provide a sample of the potential uses of electrical micro-discharges in manufacturing techniques and sensing modalities, and it seems possible that a number of applications can benefit from the proper development of this

technology. The general challenges facing researchers include spatial, temporal, and energy control of the micro-discharges, along with power-efficient methods to generate and use them. While there is much work to be done, lessons learned in other research domains – ranging from conventional plasmas and EDM technology, to radiation sensors and wireless communication – can be brought to bear, making this a rich topic for interdisciplinary research.

### Acknowledgements

The author is very grateful to many students and colleagues for their valuable contributions to this effort: Chester Wilson, Kenichi Takahata, Tao Li, Bhaskar Mitra, Christine Eun, Mark Richardson, Kensall Wise, and Andrew DeHennis.

### REFERENCES

- [1] M.A. Lieberman and A.J. Lichtenberg, *Principles of Plasma Discharges and Materials Processing*, J. Wiley, New York, 1994
- [2] J.A. Hopwood, "A Microfabricated Inductively Coupled Plasma Generator," *J. Microelectromechanical Systems*, 9(3), Sept. 2000, pp. 309-313
- [3] C.G. Wilson, Y.B. Gianchandani, R.R. Arslanbekov, V. Kolobov, and A.E. Wendt, "Profiling and Modeling of DC Nitrogen Microplasmas," *J. Appl. Phys.*, 94(5), pp. 2845-2851, Sept. 2003
- [4] C.G. Wilson, Y.B. Gianchandani, "Silicon micromachining using in situ DC microplasmas," *J. Microelectromechanical Systems*, 10(1), March 2001, pp. 50-54
- [5] C.G. Wilson, Y.B. Gianchandani, "Room Temperature Deposition of Silicon by Arrayed DC Microplasmas," *Intl. Conference on Micro Electro Mechanical Systems (MEMS 04)*, Maastricht, The Netherlands, Jan. 2004, pp. 765-768
- [6] T. Masaki, K. Kawata, T. Masuzawa, "Micro Electro-Discharge Machining and Its Applications," *Intl. Workshop on Micro Electro Mechanical Systems (MEMS '90)*, Napa Valley, California, pp. 21-26, February 1990
- [7] T. Masuzawa, M. Fujino, K. Kobayashi, T. Suzuki, N. Kinoshita, "Wire Electro-Discharge Grinding for Micro-Machining," *Ann. CIRP*, v. 34, pp. 431-434, 1985
- [8] W. Ehrfeld, H. Lehr, F. Michel, A. Wolf, "Micro Electro Discharge Machining as a Technology in Micromachining," *Proc., SPIE's Symp. Micromachining and Microfabrication*, Austin, Texas, v. 2879, pp. 332-337, October 1996
- [9] K. Takahata, N. Shibaike, H. Guckel, "A Novel Micro Electro-Discharge Machining Method Using Electrodes Fabricated by the LIGA Process," *Intl. Conf. on Micro Electro Mechanical Systems (MEMS '99)*, Orlando, pp. 238-243, January, 1999
- [10] K. Takahata, Y.B. Gianchandani, "Batch mode micro-electro-discharge machining," *J. Microelectromechanical Systems*, 10(1), pp. 102-110, Feb. 2002
- [11] K. Takahata, Y.B. Gianchandani, "A Planar Micro-Electro-Discharge Machining Process for Coronary Artery Stents," *J. Microelectromechanical Systems*, 13(6), pp. 933-9, Dec. 2004
- [12] K. Takahata, Y.B. Gianchandani, K.D. Wise, "Micromachined Antenna Stents and Cuffs for Monitoring Intraluminal Pressure and Flow," *J. Microelectromechanical Systems*, in press
- [13] M.A. Fonseca, M.G. Allen, J. Kroh, J. White, "Flexible wireless passive pressure sensors for biomedical applications," *Solid-State Sensors, Actuators and Microsystems Workshop (Hilton Head '06)*, S. Carolina, June '06, pp. 37-42
- [14] T. Li, R.Y. Gianchandani, Y.B. Gianchandani, "A Bulk PZT Microsensor for In-Situ Tissue Contrast Detection During Fine Needle Aspiration Biopsy of Thyroid Nodules," *Intl. Conf. on Micro Electro Mechanical Systems (MEMS 06)*, Istanbul, Jan. '06, pp. 12-15
- [15] T. Li, Y.B. Gianchandani, "A Micromachining Process for Die-Scale Pattern Transfer in Ceramics and its Application to Bulk Piezoelectric Actuators," *J. Microelectromechanical Systems*, 15(3), pp. 605-612, June 2006
- [16] C.G. Wilson, Y.B. Gianchandani, "Spectral Detection of Metal Contaminants in Water Using an On-Chip Microglow Discharge," *IEEE Trans. on Electron Devices*, 49(12) pp. 2317-22, Dec. 2002
- [17] M.E. Zorn, C.G. Wilson, Y.B. Gianchandani, M.A. Anderson, "Detection of Aqueous Metals Using a Microglow Discharge Atomic Emission Sensor," *Sensors Letters*, vol. 2, no. 3,4, pp. 179-185, Sept.-Dec. 2004
- [18] L. Que, C.G. Wilson, Y.B. Gianchandani, "Microfluidic Electrodischarge Devices with Integrated Dispersion Optics for Spectral Analysis of Water Impurities," *J. Microelectromechanical Sys.*, 14(2), pp. 185-191, April 2005
- [19] B. Mitra, C.G. Wilson, L. Que, P. Selvaganapathy, Y.B. Gianchandani, "Microfluidic Discharge-Based Optical Sources for Detection of Biochemicals," *Lab-on-a-Chip (IOP)*, 6(1), pp. 60-65, January 2006
- [20] S. Taylor, B. Srigengan, J.R. Gibson, D. Tindall, R. Syms, T.J. Tate, M.M. Ahmad, "A Miniature Mass Spectrometer for Chemical and Biological Sensing," *Proc. of the SPIE 4036*, 2000, pp 187-193
- [21] R.A. Miller, E.G. Nazarov, G.A. Eiceman, A.T. King, "A MEMS Radio-Frequency Ion Mobility Spectrometer for Chemical Vapor Detection," *Sensors and Actuators A*, (A91) 3, July 2001, pp. 301-12
- [22] J.A. Hopwood, "A Microfabricated Inductively Coupled Plasma Generator," *J. Microelectromechanical Systems*, 9(3), Sept. 2000, pp. 309-13
- [23] T. Cserfalvi, P. Mezei, "Emission Studies on a Glow-Discharge in Atmospheric Air Using Water as a Cathode," *J. Phys. D (Appl. Phys.)*, 26, 1993, pp. 2184-2188
- [24] R.K. Marcus, W.C. Davis, "An Atmospheric Pressure Glow Discharge Optical Emission Source for the Direct Sampling of Liquid Media," *Anal. Chem.*, 73, 2001 pp. 2903-2910
- [25] G. Jenkins, A. Manz, "Optical Emission Detection of Liquid Analytes Using a Micro-Machined DC Glow Discharge Device at Atmospheric Pressure," *Proc. Micro Total Analysis Systems*, 2001, pp. 349-350
- [26] B. Mitra, B. Levey, T.-C. Fung, Y.B. Gianchandani, "A Handheld Microdischarge Spectroscopy System for High-Speed Chemical Analysis of Gaseous and Liquid Samples," *Intl. Conference on Micro Electro Mechanical Systems (MEMS '06)*, Istanbul, Turkey, Jan. '06, pp. 554-7
- [27] B. Mitra, Y.B. Gianchandani, "The Micromachined FlashFET: A Low-Power, Three-Terminal Device For High Speed Detection of Vapors at Atmospheric Pressure," *Intl. Conference on Micro Electro Mechanical Systems (MEMS 05)*, Miami, FL, Jan. '05, pp. 794-7
- [28] J.A. Kemmer, "Silicon detectors for nuclear radiation," *Intl. Conf. on Solid-State Sensors and Actuators, (Transducers)* 1987, pp. 252-7
- [29] M. Wada, J. Suzuki, Y. Ozaki, "Cadmium telluride  $\beta$ -ray detector," *Intl. Conf. on Solid-State Sensors, Actuators, and Microsystems, (Transducers)* 1987, pp. 258-261
- [30] R. Wunstorff, "Radiation hardness of silicon detectors: current status," *IEEE Transactions on Nuclear Science*, (44) 3, June 1997 pp. 806-14
- [31] E. Bertolucci, M. Conti, G. Mettivier, M.C. Montesi, P. Russo, "BETAview: A digital  $\beta$ -Imaging system for dynamic studies of biological phenomena," *Nuclear Instruments and Methods*, A381, 1996 pp. 527-530
- [32] G.F. Knoll, *Radiation Detection & Measurement*, J. Wiley, 2000
- [33] C.G. Wilson, C.K. Eun, Y.B. Gianchandani, "D-MicroGeiger: A Microfabricated Beta-Particle Detector with Dual Cavities for Energy Spectroscopy," *Intl. Conference on Micro Electro Mechanical Systems (MEMS '05)*, Miami, FL, Jan. '05, pp. 622-5
- [34] C.E. Eun, R. Gharpurey, Y.B. Gianchandani, "Controlling Ultra Wide Band Transmissions from a Wireless Micromachined Geiger Counter," *Intl. Conference on Micro Electro Mechanical Systems (MEMS 06)*, Istanbul, Turkey, Jan. '06, pp. 570-3
- [35] C.E. Eun, R. Gharpurey, Y.B. Gianchandani, "A Magnetically Enhanced Wireless Micro-Geiger Counter," *Solid-State Sensors, Actuators, and Microsystems Workshop (Hilton Head '06)*, S. Carolina, June '06, pp. 236-9